Turbulence Properties of an Axisymmetric Separation-and-Reattaching Flow

M. Kiya,* O. Mochizuki,† H. Tamura,‡ T. Nozawa,§ R. Ishikawa,§
and K. Kushioka§
Hokkaido University, Sapporo, Japan

The time-mean and root-mean-squared values, the integral time scale, the phase velocity, and the longitudinal and circumferential length scales of the velocity and the surface-pressure fluctuations are presented for a separation-and-reattaching flow formed by the boundary-layer separation at the leading edge of a blunt circular cylinder at Reynolds numbers of the order of 10^5. The cross correlations of the surface-pressure fluctuations suggested that the flow in the reattachment region of the separated shear layer has a cellular structure. A phase-averaging measurement of the reverse-flow intermittency revealed an aspect of the spatial extent of the flow unsteadiness in the reattachment region.

Introduction

A SEPARATION-AND-REATTACHING flow is a region of flow associated with the boundary-layer separation from and reattachment onto a solid surface. In the present paper, this will be referred to as a separation bubble. At high Reynolds numbers, separation-bubble flows are turbulent and characterized by rolled-up vortices that interact with the solid surface. Fundamental separation bubbles studied so far are flow downstream of a backward-facing step; flow downstream of the leading edge of a blunt plate; flow downstream of the leading edge of a blunt circular cylinder; and flow behind a normal plate with a long splitter plate. Reviews[1-5] on these separation bubbles are published that contain extensive lists of references.

Among the four fundamental separation bubbles, the second and third are the most fundamental ones in the sense that the number of governing parameters is minimal. The turbulence structures of the second configuration are rather extensively studied,[6-8] whereas those of the third configuration have not yet been obtained to the same extent.[9-12] The purpose of this paper is to present results on turbulence properties of the third configuration, i.e., the axisymmetric separation bubble of a blunt circular cylinder.

The papers of Ota et al.[9-11] present the time-mean velocities, surface pressure, and Reynolds stresses measured by conventional hot-wire probes. Rolled-up vortices are responsible for the high level of Reynolds stresses, pressure fluctuations, and heat and mass transfer in the second half of the separation bubbles. Information on the rolled-up vortices is essential for the understanding of turbulence properties, especially in the reattachment region of the separated shear layer. Sigurdson[12] and Sigurdson and Roshko[13] demonstrate that the rolled-up vortices can be controlled by introducing periodic disturbances immediately downstream of the separation edge.

Experimental Apparatus and Method

Figure 1 illustrates a definition of the flow configuration. Experiments were performed in a closed-return wind tunnel with a working section 1.2-m high, 1.5-m wide, and 6.0-m long. The freestream turbulence level was $<0.2\%$ at a speed of 12.0–15.0 m/s. The acoustic pressure level measured near an air breather at the end of the test section was 0.8–1.2 Pa in the same range of speed. No significant peaks were found in the acoustic pressure spectrum. The ceiling of the working section was slightly curved to eliminate the longitudinal pressure gradient of the main stream.

The blunt circular cylinder tested, which was manufactured from acrylic resin pipes, was 0.200 m in diameter, 0.5-cm thick, and 2.0-m long; its leading edge was right angled. The cylinder was installed into the working section along its central axis, being fixed by four piano wires 0.9 mm in diameter at three longitudinal positions $x/d = 2.3$, 7.0, and 9.5, where d is the diameter of the cylinder. Since the length of the cylinder was more than six times the length of the separation bubble x_R, the unsteady separated flow at the trailing edge of the test cylinder was assumed to have negligible effects on the leading-edge separation bubble. The area of the cylinder projected on to a plane normal to the x direction was as low as 1.7% of that of the working section; thus, the blockage effect of the working section was neglected.

An exact alignment of the cylinder was found by matching pressures recorded on four tappings located along the circumference with an angle 90 deg in the middle ($x/x_R = 0.46$) and downstream ($x/x_R = 1.24$) of the separation bubble. The circumferential deviation of the time-mean surface pressure $P < \pm 0.003\ (\rho U_\infty^2/2)$, where ρ is the density and U_∞ is the main-flow velocity, and that of the rms surface pressure coefficient was $< \pm 0.007\ (\rho U_\infty^2/2)$. The time-mean longitudinal velocity U in the outer region of the separated shear layer, which was measured by a single I-wire probe, was uniform within $\pm 0.025 U_\infty$, whereas the rms values of the longitudinal velocity fluctuation u' were uniform within $\pm 10\%$ of its maximum value at the center of the shear layer. Thus, the time-mean flow in the separation bubble had good axisymmetry.

The test cylinder had a number of pressure taps, which were separately connected to a semiconductor strain-gauged pressure transducer (type PD104K manufactured by Toyoda Kouki Co., Ltd.), with a small cavity between the pressure tap and the diaphragm of the transducer. The sensitivity of the pressure transducers was 2.04×10^{-3} mV/Pa. The gain factor of the pressure transducers was found to be 1 ± 0.06 for frequencies less than approximately 500 Hz by comparing pressure waveforms (produced by a loud speaker) recorded by the transducers and a standard microphone; the phase shifts between the transducers and the microphone were negligibly small.

The longitudinal velocity was measured by linearized constant-temperature, hot-wire anemometers with a single I-wire

Received Aug. 26, 1989; revision received May 29, 1990; accepted for publication June 11, 1990.

*Professor, Department of Mechanical Engineering.
†Associate Professor, Department of Mechanical Engineering.
‡Instructor, Department of Mechanical Engineering.
§Graduate Student, Department of Mechanical Engineering.

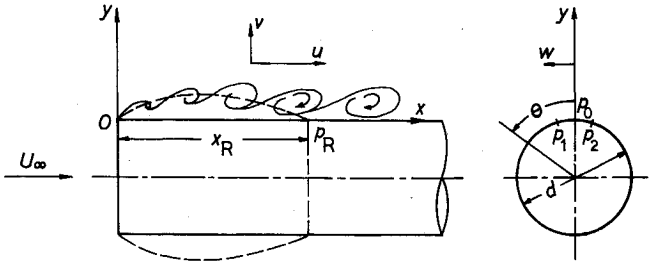

Fig. 1 Flow configuration and definition of main symbols.

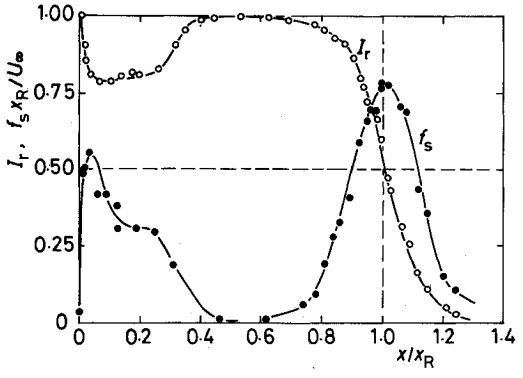

Fig. 2 Longitudinal distribution of reverse-flow intermittency I_r and frequency of switching of local-flow direction f_s measured at height $y/x_R = 0.003$; o, I_r; ●, f_s.

probe and a split-film probe. The split-film probe of diameter 0.132 mm and working length 2 mm (manufactured by Thermo-Systems, Inc.) was employed; the plane of the split was normal to the main flow, and, thus, the probe detected reversals of the local-flow direction. The split-film probe was calibrated according to Ref. 14 in a slightly modified manner.

The probes were inserted into the separation bubble with a long support of L shape. The probes were separately attached to the end of the shorter part of the support, which was 8.2-cm long and set normal to the surface of the cylinder. The longer part of the support, 47 cm in length, was set parallel to the longitudinal direction, being mounted on the traversing mechanism (inside the tunnel) that was located at least 28 cm downstream of the end of the separation bubble. This allowed the positioning of the probes to be adjusted with an accuracy of ± 0.1 mm. The possible interference between the probe and the flow was not checked, but we believe that this was negligible. The velocity and pressure fluctuations were recorded on several channels of an analog tape recorder and later analyzed by a computer to obtain statistical properties. Data recording time was 80 s; this was approximately equal to 1600 periods of shedding of large-scale vortices from the separation bubble; the data were digitized with a frequency of 800 Hz. No sensible phase lags were found between the pressure transducers and between the pressure transducer and the hot-wire and split-film probes.

The Reynolds number based on the main-flow velocity and the diameter of the cylinder was 2.0×10^5. The main-flow velocity was in a range $U_\infty = 13.5$–14.5 m/s.

Experimental Results and Discussion

Reattachment Length and Time-Mean Velocity

Throughout this paper, the time-mean length of the separation bubble x_R will be employed as a representative length and the main-flow velocity U_∞ as a representative velocity. The reattachment position was defined as a longitudinal position where the reverse-flow intermittency I_r measured near the surface was 0.5. The reverse-flow intermittency is a fraction of time during which the longitudinal velocity near the surface (which was measured by the split-film probe) is negative. This position is shown to coincide with a position of zero time-mean shear stress at the surface.[15] The reattachment length x_R was found to be $(1.60 \pm 0.01)d$ in terms of the reverse-flow intermittency measured at a height $y = 1$ mm ($y/x_R = 0.003$). The cross talk of the two films of the split-film probe[16] appears to have insignificant effects on the measured I_r because the reattachment length had the small uncertainty for several repeated measurements. The longitudinal distribution of I_r is shown in Fig. 2, which also includes the frequency of switching (denoted by f_s) of the local-flow direction from the forward to reverse flow or from the reverse to forward flow. A dip of I_r near the separation edge suggests the intermittent formation of a secondary separation bubble immersed in the main separation bubble.

Figure 3 shows the time-mean longitudinal velocity U in three typical sections in the separation bubble. The reverse-flow velocity near the surface attains a maximum value as high as $0.37U_\infty$ in the middle of the bubble. The outer edge of the separated shear layer, which is defined as a y position where the time-mean velocity U attains a maximum value, is approximately at $0.32x_R$ in the reattachment section $x/x_R = 1.0$. The center of the shear layer where $|\partial U/\partial y|$ was maximum was approximately at $0.15x_R$ in the reattachment section.

Time-Mean and Root-Mean-Squared Pressures

The time-mean and rms surface pressures are shown in Fig. 4 in terms of the pressure coefficients $c_P = 2(P - P_\infty)/(\rho U_\infty^2)$ and $c_{p'} = 2(p'^2)^{1/2}/(\rho U_\infty^2)$. The c_p profile is presented in the Roshko-Lau[17] form $(c_p - c_{p_{min}})/(1 - c_{p_{min}})$, where $c_{p_{min}}$ is the minimum value of c_p. The rms pressure coefficient attains a maximum of 0.12 slightly upstream of the reattachment line.

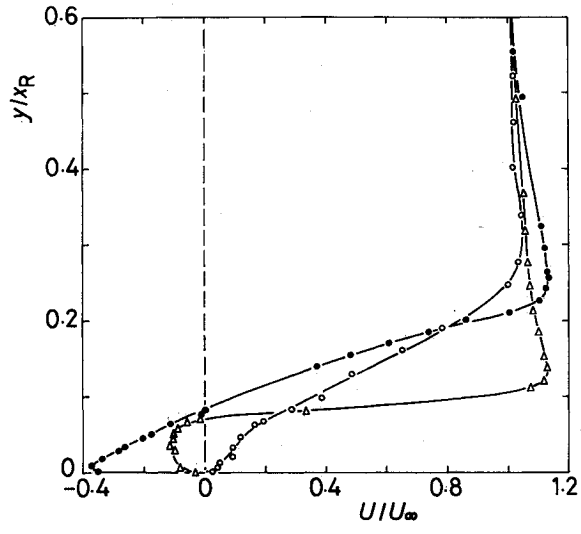

Fig. 3 Distributions of time-mean longitudinal velocity U in three representative sections: Δ, $x/x_R = 0.124$; ●, $x/x_R = 0.617$; o, $x/x_R = 1.01$.

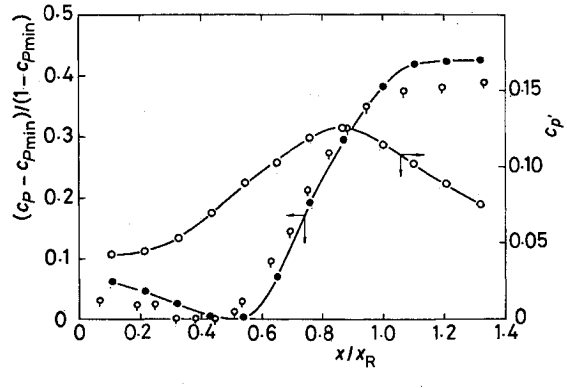

Fig. 4 Distributions of time-mean and rms surface-pressure coefficients c_p and $c_{p'}$, respectively: o, $(c_p - c_{p_{min}})/(1 - c_{p_{min}})$ by Ota.[9]

Figure 5a shows the downstream evolution of the surface-pressure spectrum $E_{p'}(f)$, f being the frequency. The spectra vary with f^{-2} near the separation edge $x/x_R = 0.11$ and in the middle of the separation bubble $0.33 < x/x_R < 0.77$. In the reattachment region $0.88 < x/x_R < 1.11$, the spectra vary with f^{-3} at high frequencies; the spectrum further downstream $x/x_R = 1.33$ seems to have a f^{-1} range. In Fig. 5b, the spectrum was multiplied by the frequency and is shown on a linear scale, whereas the frequency is on the logarithmic scale. A merit of this representation is that we can find a frequency of

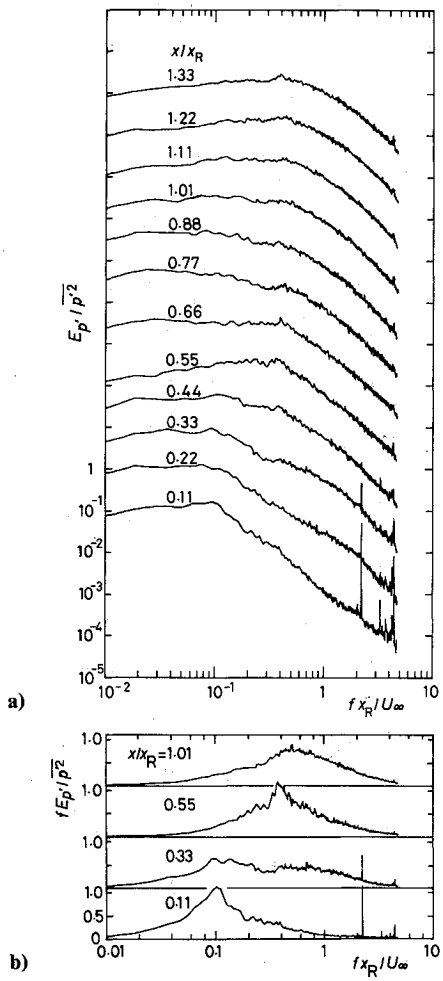

Fig. 5 Evolution of surface-pressure spectra in longitudinal direction: a) $E_{p'}/\overline{p'^2}$ in log-log plot; b) $fE_{p'}/\overline{p'^2}$ in semilog plot. Vertical scale is arbitrary.

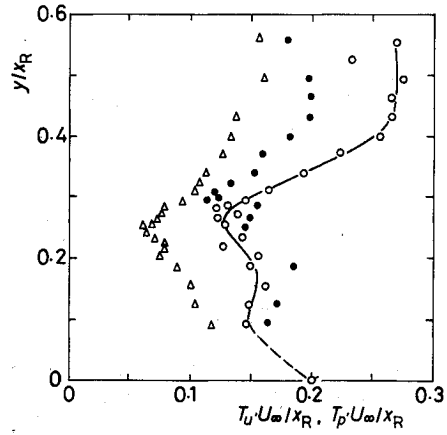

Fig. 6 Integral time scales of longitudinal-velocity and surface-pressure fluctuations in three representative sections: Δ, $x/x_R = 0.5$; o, $x/x_R = 1.0$; ●, $x/x_R = 1.5$. Flagged symbol is for $T_{p'}$ and other symbols are for $T_{u'}$. Solid and broken line is for visual aid only.

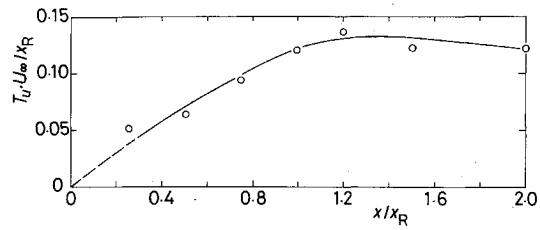

Fig. 7 Growth of minimum value of integral time scale $T_{u'}$ in longitudinal direction.

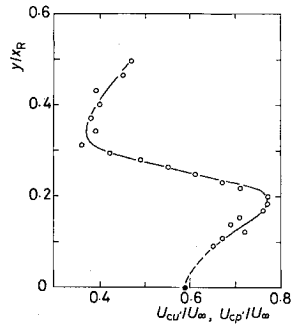

Fig. 8 Phase velocities of longitudinal-velocity and surface-pressure fluctuations in reattachment section $x/x_R = 1.0$. Solid circle is for $U_{cp'}$.

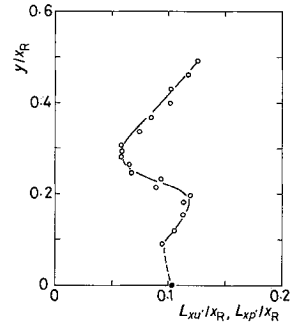

Fig. 9 Longitudinal length scales of longitudinal-velocity and surface-pressure fluctuations in reattachment section $x/x_R = 1.0$. Solid circle is for $L_{xp'}$.

the fluctuations that contain a major part of energy $\overline{p'^2}$. Two peaks of the spectra are worth noting. The first peak at a frequency $fx_R/U_\infty \cong 0.1$, which appears shortly downstream of the separation edge, is attributed to the low-frequency flapping motion of the separated shear layer.[1,6,7,18]

The second peak at a frequency $fx_R/U_\infty \cong 0.6$ reflects the shedding of large-scale vortices from the separation bubble; this frequency is hereinafter referred to as f_v. The pseudoperiodic formation and shedding of the large-scale vortices are speculated to be caused by a feedback mechanism.[19] The large-scale vortex shedding and the low-frequency flapping motion are probably inherent properties of the separation bubbles formed by the separation from a salient edge, although Ruderich and Fernholz[15] found no low-frequency component for the separation bubble behind a normal plate with a long splitter plate.

Correlation and Integral Scales

The autocorrelation coefficients of the velocity u' and the surface pressure p' were measured at a number of positions in the separation bubble and used to estimate the integral time scales $T_{u'}$ and $T_{p'}$. The measurement of u' was made by the single I-wire probe, so that it was limited to the outer region of the shear layer $y/x_R > 0.1$ where the reverse-flow intermittency was low. The integral time scales are shown in Fig. 6. The y position where $T_{u'}$ attains a minimum is close to the edge of the shear layer, whereas the position where $T_{u'}$ attains

a maximum is far beyond the intermittently turbulent region. Thus, it is reasonable to take the minimum time scale as a representative time scale; this is plotted as a function of the longitudinal distance in Fig. 7.

Figure 8 shows the phase velocities of the velocity and surface-pressure fluctuations, which are denoted by $U_{cu'}$ and $U_{cp'}$. The phase velocity $U_{cu'}$ was obtained in terms of the cross correlation of u' measured by two single hot-wire probes arranged along the longitudinal direction with a small distance $\Delta x = 0.4$ cm at various heights above the surface. The phase velocity $U_{cp'}$ was obtained in the same way in terms of the surface-pressure fluctuations detected by two pressure transducers separated in the longitudinal direction with a distance $\Delta x = 1.5$ cm. A large change of the time scale $T_{u'}$ and the phase velocity $U_{cu'}$ in the y direction is perhaps a result of distortion of vortical structures during their motion. The longitudinal length scales of the fluctuations, which are denoted by $L_{xu'}$ and $L_{xp'}$, were defined as the product of the phase velocity and the time scale. The length scales are shown in Fig. 9 for the reattachment section. This figure indicates that the length scale of the pressure $L_{xp'}$ can be taken as an average value in the shear layer. This value is approximately equal to $0.1x_R$.

The cross correlation coefficient of the surface-pressure fluctuations at two positions along the reattachment line, $R_{p'p'}(\Delta\theta)$, $\Delta\theta$ being the angle between the two positions, is shown in Fig. 10. This was measured by two pressure taps located immediately upstream ($x/x_R = 0.997$) and downstream ($x/x_R = 1.003$) of the reattachment line; in this experiment, the test cylinder was divided into two parts at the reattachment line and connected by a screw device to have an arbitrary value of the angle $\Delta\theta$. The circumferential length scale (denoted by $L_{O_{p'}}$) estimated from the cross correlation was $0.1x_R$, and, thus, the aspect ratio $L_{O_{p'}}/L_{xp'}$ of the large-scale vortices in the reattachment region was approximately unity.

The cross correlation appears to have several maxima, minima, and plateaus. These are not due to experimental errors but probably reflect a cellular pattern of the vortical structures

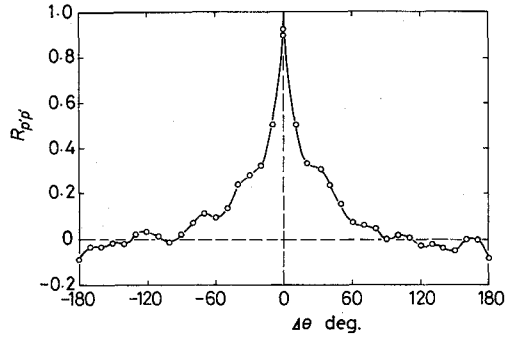

Fig. 10 Circumferential cross correlation coefficient $R_{p'p'}$ on reattachment line.

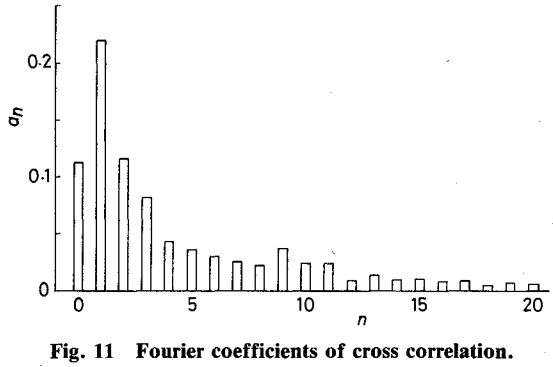

Fig. 11 Fourier coefficients of cross correlation.

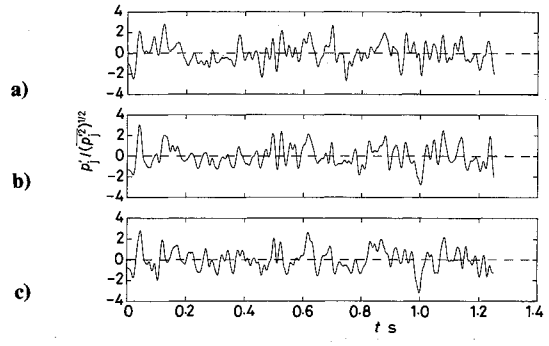

Fig. 12 Sample records of simultaneous surface-pressure waveforms $p_{j'}$ at three positions separated by 12 deg on reattachment line: a) $j = 1$, b) $j = 0$, c) $j = 2$.

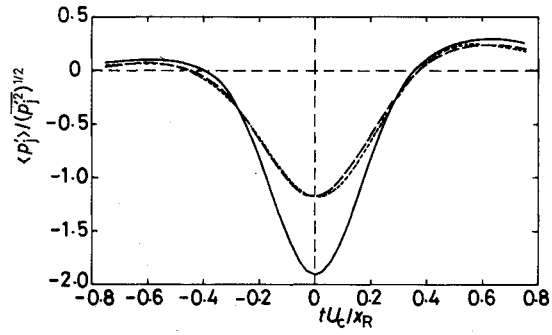

Fig. 13 Phase-averaged, surface-pressure fluctuations for valleys of p_0': --, $j = 0$; ——, $j = 1$; ... $j = 2$.

in the reattachment region. A Fourier analysis of the cross correlation in the form

$$R_{p'p'}(\Delta\theta) = \sum_{n=0}^{20} a_n \cos(n\Delta\theta)$$

revealed that the ninth coefficient a_9 was a maximum, as shown in Fig. 11. The authors' interpretation of this result is that the flow along the reattachment line has a cellular structure with nine cells. The nine-cell structure is not inconsistent with the just mentioned value of the circumferential length scale $L_{\theta_{p'}}$.

Phase-Averaged Reverse-Flow Intermittency

It is reasonable to assume that the high level of the surface-pressure fluctuations in the reattachment region of the separated shear layer is produced by the motion of the large-scale vortices impinging on the surface. Thus, the unsteady nature of flow associated with the large-scale vortices can be obtained by a phase-averaging technique that employs the surface-pressure waveforms on the reattachment line as conditioning signals.

The pressure waveforms measured at three positions along the reattachment line were employed as the conditioning signals. In view of the fact that a particular cell extends, on the average, over an angle 40 deg, the three positions were separated by an angle $\Delta\theta = 12$ deg, being assigned azimuthal angles $\theta = +12$, 0, and -12 deg. Pressure fluctuations at these positions are respectively denoted by p_1', p_0', and p_2', as shown in Fig. 1. These pressures were well correlated, the cross correlation coefficients $\overline{p_0'p_1'}/(\overline{p_0'^2}\ \overline{p_1'^2})^{1/2}$ and $\overline{p_0'p_2'}/(\overline{p_0'^2}\ \overline{p_2'^2})^{1/2}$, being approximately 0.6, as can be seen in Fig. 10.

Sample records of the three surface pressures are shown in Fig. 12. These signals were low-pass filtered with a cutoff frequency of 50 Hz, which is approximately 2.5 times the vortex shedding frequency $f_v \cong 20$ Hz. We intended to obtain the reverse-flow intermittency structure that was symmetrical with respect to the plane $\theta = 0$ deg. It is possible that real large-scale structures may not have such symmetry, as recently

found for turbulence-producing events in a turbulent channel flow.[20] We have no information on patterns of the surface-pressure fluctuations associated with such asymmetrical structures.

The sample records of Fig. 12 have peaks and valleys with widely distributed heights and depths. The peaks and valleys are perhaps an indication of the three-dimensionality of the large-scale vortices: Since the surface-pressure fluctuation at a particular position on the reattachment line is expected to attain a valley when a large-scale vortex is above the position, the depth of the valleys is probably a measure of the circumferential distance between the position and an effective center of the vortices. On the other hand, a peak of the surface-pressure fluctuation is expected to appear when the position of the pressure measurement is located in the middle of two consecutive large-scale vortices. This consideration led to the idea that an aspect of the large-scale vortices can be obtained by phase averaging the velocities in the reattachment region with respect to the time when the valleys deeper (or the peaks higher) than a threshold level were recorded.

The phase averaging was made by taking the following two steps: 1) the time when valleys or peaks of p_0' that satisfied the condition

$$|p_0'|/(p_0'^2)^{1/2} \geq C_1 \qquad (1)$$

was found, being denoted by t_V and t_p, respectively; 2) if, at the time t_V or t_p, the pressure p_1' and p_2' satisfied the condition

$$p_j'/p_0' \leq \langle p_j' \rangle / \langle p_0' \rangle + C_2 \qquad (j = 1 \text{ and } 2) \qquad (2)$$

then the time t_V or t_p was employed as the origin of time to phase average the velocity field in the reattachment region. Here, $\langle\ \rangle$ implies the phase-averaged value of the pressures at the valleys or the peaks of p_0'.

After a number of preliminary data processings, the value of C_1 was chosen as 1.3. With this value of C_1, the frequency of detecting the valleys or the peaks was approximately 8 Hz, which was approximately 40% of the vortex-shedding frequency f_v. Figure 13 shows the phase-averaged pressure fluctuations $\langle p_0' \rangle$, $\langle p_1' \rangle$, and $\langle p_2' \rangle$ for the valleys. The phase-averaged pressures for the peaks were approximately antisymmetrical to those of Fig. 13 with respect to the origin.

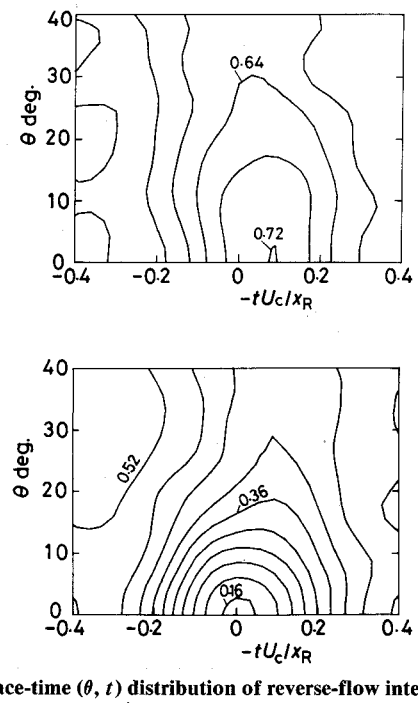

Fig. 14 Space-time (θ, t) distribution of reverse-flow intermittency I_r for peaks and valleys of p_0' measured at height $y/x_R = 0.003$. Contour interval is 0.04: a) valleys; b) peaks.

The probability density of $\Delta(p_j'/p_0') = p_j'/p_0' - \langle p_j' \rangle / \langle p_0' \rangle$ ($j = 1$ and 2) had a large dispersion, so that it was difficult to find a particular threshold level C_2. After comparing results of a number of preliminary data processings, a value of $C_2 = 0.2$ was chosen. This was because the right side of Eq. (2) should be smaller than unity in view of the assumed symmetry of the large-scale vortices. The values of $\langle p_j' \rangle / \langle p_0' \rangle$ at the time $t = 0$ are approximately 0.6 as seen in Fig. 13, so that the right side of Eq. (2) < 0.8 at the time t_V or t_p for the previous value of C_2. The frequency of detecting the valleys or the peaks of the pressures p_0', p_1', and p_2' that simultaneously satisfied Eqs. (1) and (2) was, on the average, 5 Hz, which is approximately equal to $f_v/4$. We did not systematically change values of C_1 and C_2, but another combination $C_1 = 1.5$ and $C_2 = 0.3$ produced insignificant changes of patterns for their original combination.

The result is shown in Fig. 14, which is the distributions of the reverse-flow intermittency $\langle I_r \rangle$ measured at a height $y/x_R = 0.003$. The flow near the cylinder surface is seen to be generally reversed for the valleys of p_0', whereas for the peaks of p_0', the flow near the surface is generally in the forward direction. The circumferential extent of contours of I_r in Fig. 14b is not inconsistent with the nine-cell structure of the flow in the reattachment region. It is hoped that well-controlled experiments in the near future will disclose more detailed structures.

Conclusions

This paper has described turbulence properties of the leading-edge separation bubble of a blunt circular cylinder aligned to a uniform main flow at a Reynolds number of the order of 10^5. Main results of this study can be summarized as follows.

1) Distributions of the time-mean and rms surface pressures are presented at several positions in the separation bubble.

2) The integral time scale, the phase velocity, and the longitudinal length scale of the longitudinal velocity and the surface-pressure fluctuations are presented.

3) Flow in the reattachment region appears to have a cellular structure with nine cells. The phase-averaged reverse-flow intermittency in the reattachment region demonstrates the spatial extent of the unsteady-flow region associated with the large-scale vortices.

4) Flow in the separation bubble has two typical frequencies: one is associated with the low-frequency flapping motion of the separated shear layer, and the other is associated with the shedding of the large-scale vortices from the separated zone.

Acknowledgment

This study was supported by the Grant-in-Aid for Scientific Studies (No. 01460108) from the Ministry of Education, Science and Culture of Japan.

References

[1]Eaton, J. K., and Johnston, J. P., "A Review of Research on Subsonic Turbulent Flow Reattachment," *AIAA Journal,* Vol. 19, No. 9, 1981, pp. 1093–1100.

[2]Simpson, S. L., "Two-Dimensional Turbulent Separated Flow," *AGARDograph* 287, Vol. 1, June 1985.

[3]Simpson, R. L., "Turbulent Boundary Layer Separation," *Annual Review of Fluid Mechanics,* Vol. 2, 1989, pp. 205–234.

[4]Kiya, M., "Structure of Flow in Leading-Edge Separation Bubbles," *Boundary-Layer Separation,* edited by F. T. Smith and S. N. Brown, Springer-Verlag, Berlin, 1987, pp. 57–71.

[5]Kiya, M., "Separation Bubbles," *Theoretical and Applied Mechanics,* edited by P. Germain, M. Piau, and D. Caillerie, Elsevier, Amsterdam, North Holland, 1989, pp. 173–191.

[6]Kiya, M., and Sasaki, K., "Structure of a Turbulent Separation Bubble," *Journal of Fluid Mechanics,* Vol. 137, 1983, pp. 83–113.

[7]Cherry, N. J., Hillier, R., and Latour, M.E.M.P., "Unsteady Measurements in a Separated and Reattaching Flow," *Journal of Fluid Mechanics,* Vol. 144, 1984, pp. 13–46.

[8]Kiya, M., and Sasaki, K., "Structure of Large-Scale Vortices and

Unsteady Reverse Flow in the Reattaching Zone of a Turbulent Separation Bubble," *Journal of Fluid Mechanics,* Vol. 154, 1985, pp. 463–491.

[9]Ota, T., "An Axisymmetric Separated and Reattached Flow on a Longitudinal Blunt Circular Cylinder," *Journal of Applied Mechanics,* Vol. 42, No. 2, 1975, pp. 311–315.

[10]Ota, T., and Motegi, H., "Turbulence Measurements in an Axisymmetric Separated and Reattached Flow Over a Longitudinal Blunt Circular Cylinder," *Journal of Applied Mechanics,* Vol. 47, No. 1, 1980, pp. 1–6.

[11]Ota, T., Kon, N., Hatakeyama, S., and Sato, S., "Measurements of Turbulent Shear Stress and Heat Flux in an Axisymmetric Separated and Reattached Flow Over a Longitudinal Blunt Circular Cylinder," *Bulletin of the JSME,* Vol. 23, No. 184, 1980, pp. 1639–1645.

[12]Sigurdson, L. W., "The Structure and Control of a Turbulent Reattaching Flow," Ph.D. Dissertation, California Inst. of Technology, Pasadena, CA, 1986.

[13]Sigurdson, L. W., and Roshko, A., "The Structure and Control of a Turbulent Reattaching Flow," *Turbulence Management and Relaminarization,* edited by H. W. Liepmann and R. Narashimha, Springer-Verlag, Berlin, 1988, pp. 497–514.

[14]"TSI Split Film Sensor Calibration and Applications," *Technical Bulletin* TB20, Thermo-Systems, Inc., Minneapolis, MN.

[15]Ruderich, R., and Fernholz, H. H., "An Experimental Investigation of a Turbulent Shear Flow with Separation, Reverse Flow and Reattachment," *Journal of Fluid Mechanics,* Vol. 163, 1986, pp. 283–322.

[16]Ho, C.-M., "Response of a Split Film Probe Under Electrical Perturbations," *Review of Scientific Instruments,* Vol. 58, No. 8, 1982, pp. 1240–1245.

[17]Roshko, A., and Lau, J. C., "Some Observations on Transition and Reattachment of a Free Shear Layer in Incompressible Flow," *Proceedings of the 1965 Heat Transfer and Fluid Mechanics Institute,* edited by A. F. Charwat, Stanford University Press, Stanford, CA, 1965, pp. 157–167.

[18]Castro, I. P., and Haque, A., "The Structure of a Turbulent Shear Layer Bounding a Separation Region," *Journal of Fluid Mechanics,* Vol. 179, 1987, pp. 439–468.

[19]Gharib, M., and Roshko, A., "The Effect of Flow Oscillations on Cavity Drag," *Journal of Fluid Mechanics,* Vol. 177, 1987, pp. 501–530.

[20]Guezcennec, Y. G., Piomelli, U., and Kim, J., "On the Shape and Dynamics of Wall Turbulence in Turbulent Channel Flow," *Physics of Fluids* A, Vol. 1, No. 4, 1989, pp. 764–766.